Highly biocompatible rGO-TiO2 nanomaterials effectively enhance the phycocyanin yield of Arthrospira platensis FACHB-314 under visible light conditions

PAN XIONG[1] and Siming Xu[2]

[1]Ludwig Maximilians University Munich Department of Biology I
[2]Xiamen University

October 31, 2022

Abstract

Human health is burdened by diverse range diseases, particularly chronic diseases. Free radicals and other oxidants are implicated in development of those diseases as free radicals induced oxidative stress. The antioxidants are salient substances that involve maintaining a normal long life by scavenging the free radicals in the body. Phycocyanin is free radicals' scavenger with ability to find and tackle the side effects of free radicals; the phycocyanin also possesses other physiological and pharmaceutical properties. This research aimed at evaluating the effectiveness of TiO2 nanoparticles, and reduced graphene oxide titanium dioxide nanoparticles (herein after referred to rGO-TiO2 nanoparticles) under visible light conditions to boost the accumulation of phycocyanin in Arthrospira (Spirulina) platensis (FACHB-314) cells. The experimental results indicated that the both nanoparticles exhibited high phycocyanin content accumulation compared to the control group. Under optimized visible light conditions of 165 µmol/m2/s wavelength and continuous lighting with white lights, the phycocyanin content of 80.3 mg/g and maximum yield of phycocyanin production were 97.16 mg/L in the rGO-TiO2 nanoparticles culture; 55.7 mg/g and 81.88 mg/L in the TiO2 nanoparticles culture, compared to 75.5 mg/g and 81.86 in the control culture. The maximum dry weight biomass cells were observed under the control group compared the experimental conditions. These research results indicate that rGO-TiO2 nanoparticles have potential commercial applications due to the excellent properties, and can be used in A. platensis and other microalgae cultivation to optimize productivity.

Highly biocompatible rGO-TiO_2 nanomaterials effectively enhance the phycocyanin yield of Arthrospira platensis*FACHB-314* under visible light conditions

Pan Xiong [1 *], Siming Xu [2]

[1] Plant Molecular Biology, Faculty of Biology, Ludwig-Maximilians-University (LMU)Munich, Martinsried-Planegg, D-82152 Munich, Germany

[2] Department of Chemical and Biochemical Engineering, College of Chemistry and Chemical Engineering, Xiamen University, 361005 Xiamen, China

*Corresponding author:

Dr. Pan Xiong

Tel: +49 (0)89-2180 74681; fax: +49 (0)89-2180 74563

E-mail: *P.Xiong@lmu.de*

Abstract

Human health is burdened by a diverse range of diseases, particularly chronic diseases. Free radicals and other oxidants are implicated in the development of those diseases as free radicals induced oxidative stress. Antioxidants are salient substances that involve maintaining a normal long life by scavenging the free radicals in the body. Phycocyanin is free radicals' scavenger with the ability to find and tackle the side effects of free radicals; phycocyanin also possesses other physiological and pharmaceutical properties.

This research aimed at evaluating the effectiveness of TiO_2 nanoparticles, and reduced graphene oxide titanium dioxide nanoparticles (hereinafter referred to rGO-TiO_2nanoparticles) under visible light conditions to boost the accumulation of phycocyanin in *Arthrospira (Spirulina) platensis*(*FACHB-314*) cells. The experimental results indicated that both nanoparticles exhibited high phycocyanin content accumulation compared to the control group. Under optimized visible light conditions of 165 μmol/m^2/s wavelength and continuous lighting with white lights, the phycocyanin content of 80.3 mg/g and maximum yield of phycocyanin production was 97.16 mg/L in the rGO-TiO_2nanoparticles culture; 55.7 mg/g and 81.88 mg/L in the TiO_2 nanoparticles culture, compared to 75.5 mg/g and 81.86 in the control culture. The maximum dry-weight biomass cells were observed under the control group compared to the experimental conditions. These research results indicate that rGO-TiO_2 nanoparticles have potential commercial applications due to their excellent properties, and can be used in*A. platensis* and other microalgae cultivation to optimize productivity.

Keywords: rGO-TiO_2, *FACHB-314* , phycocyanin, nanoparticles, algae

1. Introduction

As part of the human diet, *FACHB-314* is one of the long-used cyanobacteria, and it is also the first batch of algae bacteria to be industrialized using modern biotechnology (Almomani, 2020; Ambati et al., 2019). *FACHB-314* belongs to blue-green prokaryotic microalgae with photosynthesis, filamentous, spiral, and multicellular blue-green microalgae, larger than other types of microalgae (Nematian et al., 2020; Shi et al., 2020). Due to the lack of cellulose in the cell membrane (Ribeiro et al., 2021; Rosenau et al., 2021) is easily digested and absorbed by the human body (Karthikeyan et al., 2020). And it has many benefits to human health, including anti-cancer (Patel et al., 2021), antioxidant (Mustafa et al., 2021), anti-viral (Lupatini Menegotto et al., 2021; Mona et al., 2021) and anti-inflammatory (Basavarajappa et al., 2020; Grossmann et al., 2020; Hazeem et al., 2020). Therefore, it can be used to produce health foods (Keller et al., 2021), cosmetics (Hong et al., 2021b), food additives (Hong et al., 2021a) and medicines (Almomani, 2020). In addition, due to the high content of nutrients in its cells (Guo et al., 2021), it can produce more substances, such as pigments, fatty acids, vitamins, minerals, etc. (Sathasivam et al., 2019; Wang et al., 2019; Yucetepe et al., 2019), especially for the production of phycocyanin (Akter et al., 2021), which content can reach 10-20% (Rosa et al., 2019).

Phycocyanin is composed of apolipoprotein (Fu et al., 2021) and phycocyanin (Liu et al., 2019). Apolipoprotein binds to phycocyanin through ether-sulfur bonds (Li et al., 2019). The protein part is composed of the α subunit and β subunit (Karakas et al., 2019; Kashyap et al., 2019). Due to the presence of open-chain tetrapyrrole, it is an auxiliary photosynthetic pigment, and its color is dark blue (Alagawany et al., 2021; He et al., 2019). It is a non-toxic pigment protein with good water solubility (Ferreira-Santos et al., 2021), antioxidant, anti-inflammatory, neuroprotective, and liver protective effects (Ambati et al., 2019; Buchmann et al., 2019; Dalu et al., 2019). It's the research object of many scholars. In the food industry, phycocyanin is mainly used as a natural dye to replace artificial dyes that are harmful to human health (Ye et al., 2018; Zhang et al., 2018). In the medical field, the absorption and emission wavelengths are high, the fluorescence quantum yield and light stability are good, the extinction coefficient is large, and the solubility in water is high (Thirumdas et al., 2018; Wang & Lan, 2018). Therefore, based on the properties of phycocyanin, can also be used as a fluorescent label (Sengupta et al., 2018).

However, as a phycocyanin extracted from biological algae, its application has certain limitations, such as low yield and difficulty in large-scale production (Rizwan et al., 2018; Rodrigues et al., 2018). Therefore, the main method to overcome such limitations is to increase biomass (because of its higher value) and increase

the content of valuable products produced by cell metabolism (Ozkaleli & Erdem, 2018; Raji et al., 2018). In recent years, the importance of nanomaterials has greatly increased (Wang et al., 2017). Based on previous studies, titanium dioxide (TiO_2) nanoparticles (NPs) are currently one of the most widely used nanomaterials (Nguyen et al., 2018; Ozkaleli & Erdem, 2018). However, in such studies, we found that TiO_2 has a certain inhibitory and toxic effect on the growth of algae cells due to its relatively poor biocompatibility and strong cytotoxicity (Zhou et al., 2021; Zhu et al., 2021). For this, we creatively upgrade materials, Synthesized rGO-TiO_2composite nanomaterials for the co-cultivation of Spirulina.

This work fabricated highly biocompatible rGO-TiO_2nanoparticles to be used in the cultivation process of *FACHB-314* . Aims to improve the absorption and utilization of light by algae, and promote the growth of algae cells and the accumulation of photosynthesis, thereby increasing the production of phycocyanin. In the process of microalgae cultivation, increasing the production of own cells can also increase the output of phycocyanin. Developing a technology that can effectively synthesize phycocyanin in*FACHB-314* and explore the feasibility of the corresponding technology.

2. Materials and Methods

2.1. Culture conditions and Materials of FACHB-314

Spirulina *FACHB-314* was purchased from Wuhan Institute of Aquatic Plants, Chinese Academy of Sciences. Zarrouk medium (Lebron et al., 2018; Liang et al., 2018) is used as a medium for *FACHB-314*experiments, composition (g/L: $NaHCO_3$ 16.8, $NaNO_3$ 2.5, K_2SO_4 1.00, NaCl 1.00, $MgSO_4{\cdot}7H_2O$ 0.20, $FeSO_4{\cdot}7H_2O$ 0.01, K_2HPO_4 0.50, $CaCl_2{\cdot}2H_2O$ 0.04, EDTA 0.08, 1mL of trace elements. Among them, trace element composition (g/L): H_3BO_3 2.86, $MnCl_2{\cdot}4H_2O$ 1.81, $ZnSO_4{\cdot}4H_2O$ 0.22, $NaMoO_4$0.018, $CuSO_4{\cdot}5H_2O$ 0.08.

Inoculate *FACHB-314* into the reactor and put it in the smart light incubator (Khanra et al., 2018). The structure of the reactor is shown in Scheme 1. The photobioreactor is a 1 L conical flask with a bottom radius of 9 cm and a height of 20 cm. Place the photobioreactor in a smart light incubator, keep the temperature at 25°C, and continuously supply air at a ventilation rate of 0.7 vvm (Karthikeyan et al., 2018a). In an Erlenmeyer flask containing TiO_2 and rGO-TiO_2, 50 mg of nanomaterials were added for co-cultivation.

2.2. Synthesis of Nanocomposites

Figure 1 shows the specific process, rGO-TiO_2nanomaterial was prepared by the reaction of graphene oxide and tetrabutyl titanate through a hot solvent (Karthikeyan & Prabhakaran, 2018; Karthikeyan et al., 2018b). The graphene oxide was poured into isopropanol and sonicated. Then add tetrabutyl titanate, stir well, and then add 1 mL of ultrapure water to the mixed solution. After stirring for 30 minutes, it was transferred to a polytetrafluoroethylene lining and reacted at 180 °C in a blast drying oven. After 8 hours of reaction, the precipitate was centrifuged and washed several times with absolute ethanol. After drying for several hours, a small amount of black product was obtained, which is the target product of this experiment.

2.3. Determination of FACHB-314 Cell Growth

Accurately weigh the 50 ml centrifuge tube and mark it as M_0. Transfer 20 ml of algae solution and centrifuge for 10 minutes (Caporgno & Mathys, 2018). Leave the sediment and wash it several times, and finally dry it to a constant weight, weigh it as M_1, and then calculate the dry battery weight DCW (g/L) according to Eqs (1) Measure the absorbance value at 680nm using an ultraviolet-visible spectrophotometer.

The absorbance value multiplied by the dilution factor is the OD_{680} of *FACHB-314* . The relationship between battery dry weight DCW (g / L) and OD_{680} is Eqs (2):

$$DCW(g/L): \ M = 1000 \times (M1 - M0) \div 20 \ (1)$$

$$DCW(g/L) = 0.5192\mathrm{OD}_{680} \pm 0.01002(R^2 = 0.99779) \ (2)$$

2.4. Determination of Phycocyanin and Allophycocyanin

Protein extraction and determination: PB buffer is used to extract phycocyanin and allophycocyanin after repeated freezing and thawing (Hu et al., 2018). A spectrophotometer was used to determine the concentration of phycocyanin and allophycocyanin (Bhalamurugan et al., 2018). The relationship between protein concentration and absorbance is Eqs (3) (4):

$$PC(mg/mL) = (A_{620} - 0.474A_{652}) \div 5.34 \quad (3)$$

$$APC(mg/mL) = (A_{652} - 0.208A_{620}) \div 5.09 \quad (4)$$

The determination of phycocyanin content comes from the formula (5):

$$PC\ content(mg/g) = PCV/M \quad (5)$$

where V represents the volume of the PB solution of the extracted protein, and M represents the dry weight of *FACHB-314* at this concentration.

According to Eqs (6), the phycocyanin and allophycocyanin in the algae can be obtained in sequence:

$$\text{PC content} = (C1 \times V1)(C2 \times V2) \quad (6)$$

Among them, PC content represents the content of phycocyanin per unit cell dry weight (mg/g); C1 represents the concentration of two proteins (mg/ml), V1 represents the volume of phosphate buffer (ml), and C2 represents *FACHB-314* Corresponding dry cell weight (g/L); V2 represents the weighed volume of algal liquid (mL).

According to Eqs (7), the purity of phycocyanin can be obtained:

$$\text{PC production} = PC\ content \times DCW \quad (7)$$

Among them, PC content represents the content of phycocyanin per unit cell dry weight (mg/g); DCW represents the dry cell weight (g/L) of the phycocyanin content.

2.5. Morphology and Submicroscopic structure of FACHB-314

SEM and TEM were used to observe the morphology and submicroscopic structure of *FACHB-314* and nanomaterials (Benedetti et al., 2018). Micrographs were used to analyze the effects of rGO-TiO_2 and TiO_2 nanoparticles on the morphology of *FACHB-314* cells (Bajpai et al., 2018; Wils et al., 2021).

3. Results

3.1. Characterization of rGO-TiO_2Composite Materials

Figure 2 shows that GO has a strong diffraction peak at 11°, which is a characteristic peak (Zhan et al., 2017). With the reaction of GO and tetrabutyl titanate, the composite material rGO-TiO_2 is formed. There are characteristic peaks of TiO_2, 2 theta is 25.3°, 37.8°, 48.0°, 53.9°, 55.1° and 62.7°. These angles correspond to the 6 crystal planes (101), (004), (200), (105), (211), and (204) of anatase TiO_2 (Wang et al., 2017), of which the peak corresponding to the (101) crystal plane is the most. The sharpness and maximum strength indicate that the TiO_2 in the composite material is mainly anatase crystal type (Sorrenti et al., 2021; Wang et al., 2021). In this structure, the diffraction peak of graphene is also not observed. This is because the characteristic peak of graphene is at 24.5°, which is easily covered by the strong diffraction peak at 25.3° of the anatase (101) crystal plane.

From Figure 3 (a), (b), and (c), it can be shown that TiO_2 nanoparticles have been supported on a thin layer of graphene oxide. The high-resolution lattice phase analysis of the region with nanoparticles is shown in Figure 3(d). It can be observed that the interval of the lattice fringes is 0.352 nm, which corresponds to the anatase TiO_2 (101) crystal plane (Wu et al., 2017; Yung et al., 2017). The above results can indicate that the TiO_2 nanoparticles were successfully supported on the graphene oxide substrate.

Figure 4(a) shows the XPS full spectrum of GO and nanoparticles rGO-TiO_2. The full spectrum of rGO-TiO_2nanoparticles contains three elements, of which the characteristic peak of C 1s is at 284.41 eV (Shirazi

et al., 2017), the characteristic peak of Ti 2p is at 459.72 eV (Minetto et al., 2017), and the characteristic peak of O 1s is at 530.98 eV (Sendra et al., 2017). Correspondingly, the XPS full spectrum of GO contains only two elements, such as C and O. The characteristic peak of C 1s is at 286.76 eV, and the characteristic peak of O 1s is at 532.50 eV (Madeira et al., 2017). XPS high-resolution analysis was performed on the C 1s of GO and the composite nano-catalyst rGO-TiO_2. As shown in Figure 4(b), it is the high-resolution XPS spectrum of GO C 1s. In addition to the symmetrical sp^2 hybridized C-C bond at 284.82 eV, it is also observed at 288.30 eV and 289.14 eV. Peaks, these two peaks respectively correspond to epoxy C-O-C, carboxyl HO-C=O, and other oxygen-containing active groups. In the composite structure prepared with GO as the raw material, as shown in Figure 4(b), is the high-resolution XPS spectrum of the composite nano-catalyst rGO-TiO_2 with C 1s. The peak is observed at 286.08 eV in the figure, which corresponds to the C-C bond may be due to the solvothermal reaction, other oxygen-containing active groups are gradually reduced. This indicates that GO has been reduced to rGO during the synthesis process of the composite material.

3.2. Biocompatibility of composite materials and FACHB-314

We studied the effects of nanoparticles of rGO-TiO_2 on the biomass and nitrate consumption of *FACHB-314* and its cell structure or subcellular structure to determine the biocompatibility of the material with *FACHB-314* . rGO-TiO_2 composite nanoparticles were added to the *FACHB-314* culture medium to determine the change in dry cell weight and the residual nitrate content in the culture medium. *FACHB-314* cultured without nanoparticles was used as a control group. It can be observed from Figure 5 that the dry cell weight of *FACHB-314* added with composite photocatalytic nanomaterials changes relative to the blank group and the remaining nitrate content in the culture medium. Among them, Figure 5(a) shows the growth trend of the two groups of *FACHB-314* and gradually increases. On day 9, the weight of *FACHB-314* stem cells cultured on the composite photocatalytic nanomaterials reached 1.24g/L, and the blank group reached 1.36g/L. Compared with the blank group, the experimental group only changed by 8.8%. Then, the residual nitrate content in the two sets of culture media was determined. The result is shown in Figure 5(b). The residual nitrate content also tends to be consistent. Based on this, we concluded that, compared with the blank group, nanoparticle rGO-TiO_2 will not adversely affect the two indicators of *FACHB-314* biomass and remaining nitrate content.

Figure 6 shows a photomicrograph of the effect of rGO-TiO_2 and TiO_2 nanoparticles on the morphology of *FACHB-314* cells. Figure 6(a), (c), (e) shows the morphology of the three types of microalgae on the first day, (a) is a control group of *FACHB-314* under an optical microscope, (c) is*FACHB-314* with TiO_2 nanoparticles added under an optical microscope, and (e) is a control group of *FACHB-314* under an optical microscope. *FACHB-314* and rGO-TiO_2nanoparticles. The morphology of these three kinds of *FACHB-314*is normal, showing unidirectional growth and left-handed spiral arrangement. Unlike the control group, the *FACHB-314* filaments of the two experimental groups are all attached with nanoparticles, but they have no effect on the morphology and structure of *FACHB-314* . On the sixth day, the subcellular structures of the three microalgae are as follows: Figure 6 (b) is the control group *FACHB-314* under the transmission electron microscope (d) is the *FACHB-314* doped with nanoparticle TiO_2 under the transmission electron microscope, and (f) is the transmission electron microscope.*FACHB-314* doped with nanoparticles of rGO-TiO_2under the electron microscope. By observing the microstructure of the three groups of *FACHB-314* , it is found that the vegetative cells undergo two divisions during unidirectional growth, and there are obvious transfers on the transverse wall. The trichomes are wrapped in a thin sheath, and there are obvious structures at the crossing walls (Li et al., 2017; Lupatini et al., 2017). In the trichomes of the experimental group, especially under the treatment of titanium dioxide nanoparticles, the transverse wall structure of the trichomes became difficult to distinguish, the morphological abnormalities of*FACHB-314* were clearly visible, and the cell membrane and transverse wall were twisted. The horizontal wall structure in the middle disappeared. The cell shape of the control group showed a flat surface, and the cell membrane was not damaged. The mixing of*FACHB-314* and composite photocatalytic nanoparticles rGO-TiO_2 has a certain effect on the cell morphology of*FACHB-314* . For example, the horizontal wall is opaque, the cell wall is wrinkled, etc., but it still maintains the basic morphological characteristics and will not cause obvious damage to the sexual structure. The above results

indicate that rGO-TiO_2nanoparticles have good biocompatibility for the growth of*FACHB-314* .

3.3. Effects of Different wavelengths on the Growth of FACHB-314

The effect of rGO-TiO_2 nanoparticles on the growth of*FACHB-314* under different wavelengths of light was experimentally studied. Analyzed the growth data of each group of *FACHB-314* . On day 9 of the culture, the dry cell weight and biomass yield results of the three groups of *FACHB-314* are shown in Figure 7. In the medium without adding nanoparticles, the dry cell weight of*FACHB-314* under red light is only 0.58 g/L, and the dry cell weight under white light increased to 1.73 g/L. Compared with red light, the weight of stem cells has increased by nearly three times. The increment of stem cells under red right indicates that *FACHB-314*is very sensitive to light of different wavelengths, and white light is more conducive to the growth of *FACHB-314* due to the capture and absorption of light energy through the first step of photosynthesis. For the full use of the energy in sunlight, photosynthetic organisms have formed an effective light-absorbing device, which is composed of photosynthetic pigments that absorb different wavelengths during the evolution process. The device can effectively capture the energy of visible light and near-infrared light. Therefore, the decrease in the dry cell weight of *FACHB-314* can be attributed to the reduction of the wavelength range, which reduces the absorption of light energy by photosynthetic pigments and reduces the accumulation of photosynthesis in *FACHB-314* , which indicates that the growth of *FACHB-314*is slow.

The results in Table 1 show that the dry cell weight of the control group under white light is 1.73 g/L, and the stem cell yield is 0.186 g/L/d. In the medium supplemented with TiO_2nanoparticles, the dry cell weight of *FACHB-314* reached its maximum on the 9th day, which was 1.47 g/L, and the dry cell weight yield was 0.154 g/L/d. Compared with the blank control group, the dry weight of *FACHB-314* cells decreased by 15.0%, and biomass productivity decreased by 18%. The results show that TiO_2 nanoparticles have a certain inhibitory effect on the growth of *FACHB-314* . However, in the medium supplemented with rGO-TiO_2 nanoparticles, the dry cell weight of*FACHB-314* reached its maximum on the ninth day at 1.66 g/L, and the dry cell weight yield was 0.178 g/L/d. Compared with the control group, there is no significant difference between the dry cell weight of*FACHB-314* and its stem cell yield, which indicates that rGO-TiO_2 nanoparticles have no significant effect on the growth of *FACHB-314* .

Under the condition of red-light irradiation, the cell growth of*FACHB-314* was significantly inhibited, and the cell growth trend of the two experimental groups added with nanomaterials was significantly higher than that of the control group, and the biomass of the rGO-TiO_2 composite nanoparticles was the highest. Under the red-light condition, the dry cell weight of the control group was 0.58 g/L, and the dry cell weight yield was 0.053 g/L/d. Compared with the white light culture condition, the biomass of *FACHB-314*was significantly reduced by 198%. This indicated that the red wavelength light significantly inhibited the growth of *FACHB-314*cells. The dry cell weight of *FACHB-314* reached its maximum value on the ninth day of the medium supplemented with TiO_2nanoparticles, and it was 1.29 g/L, and its dry cell weight yield was 0.141 g/L/d. Compared with the control group, its dry cell weight increased by 0.71 g/L, an increase of 122.4%, and its dry cell weight yield increased by 166%. On the medium with rGO-TiO_2composite nanoparticles, the dry cell weight of *FACHB-314* reached the maximum value of 1.39 g/L on the ninth day, and the dry cell weight yield was 0.154 g/L/d. Compared with the control group, the dry cell weight increased by 0.81 g/L, an increase of 139.7%, and the dry cell weight yield increased by 191%. The above results show that under monochromatic red-light irradiation, the experimental group adding rGO-TiO_2 composite nanoparticles can significantly increase the utilization of red light in the photosynthetic system of*FACHB-314* , and thus can greatly increase the growth of*FACHB-314* cells. Compared with *FACHB-314* with TiO_2 nanoparticles added with rGO-TiO_2nanoparticles, under white light, the dry cell weight of*FACHB-314* increased by 0.19 g/L, an increase of 12.9%, and its dry cell weight yield increased by 0.024. g/L/d; under red light, its dry cell weight increased by 0.10 g/L, an increase of 7.8%, and its dry cell weight yield increased by 0.013 g/L/d. In summary, the biomass of*FACHB-314* added with rGO-TiO_2 nanoparticles was higher than that of the experimental group with TiO_2nanoparticles under two different wavelengths of light conditions.

3.4. The effect of light in different wavelength ranges on the synthesis of phycocyanin

Figure 8 shows the effects of adding nanoparticles on the intracellular accumulation of phycocyanin in *FACHB-314* under different wavelength conditions. The addition of rGO-TiO_2composite nanoparticles has a significant increase compared to other white light conditions. Table 1 shows the changes of rGO-TiO_2 composite nanoparticles on phycocyanin-related indicators of *FACHB-314* under white light. The growth curve of*FACHB-314* shows that the control group without nanoparticle culture has the highest phycocyanin content of 75.1 mg/g and the phycocyanin production of 81.86 mg/L on the sixth day of culture. In the*FACHB-314* experimental group cultured with TiO_2nanoparticles, the maximum phycocyanin content was 55.7 mg/g. Compared with the control group, the phycocyanin content decreased by 25.8%, and the intracellular phycocyanin production under this condition is 81.88 mg/L. *FACHB-314* cultured with rGO-TiO_2nanoparticles had a maximum phycocyanin content of 80.3 mg/g on the seventh day of culture. Compared with the control group, the phycocyanin content increased by 6.9%. The intracellular phycocyanin production of algae was 97.16 mg/L. Compared with the control group, the production of phycocyanin also increased by 18.7%. Compared with the *FACHB-314*cultured with TiO_2 nanoparticles, the phycocyanin content increased by 24.6 mg/g compared with the experimental group with TiO_2 nanoparticles, and the content increased by 44.2%. The production of phycocyanin also increased by 15.28 mg/g, an increase of 18.7%.

For *FACHB-314* cultured without nanoparticles, the intracellular phycocyanin content of *FACHB-314* was lower than the initial value (39.0 mg/g) under this condition, and it was gradually consumed. The maximum phycocyanin content of *FACHB-314* cultured under red light was 39.0 mg/g, and the maximum phycocyanin yield was 6.24 mg/L. Compared with white light, the phycocyanin content is reduced by 48.1%.*FACHB-314* with nanoparticles maintains a higher phycocyanin content and phycocyanin production. Among them, the rGO-TiO_2 nanoparticle *FACHB-314* has the highest phycocyanin content.

3.5. Effects of Different Light Intensities on the Growth and Phycocyanin Content of FACHB-314

The effect of rGO-TiO_2 nanoparticles on the growth of*FACHB-314* under different light intensities. The effects of high light intensity, medium light intensity, and low light intensity on the growth of *FACHB-314* by rGO-TiO_2 nanoparticles. Figure 9(a) shows that under the culture conditions of three light intensities, the largest dry cell weight is the control group cultured at 275 μmol/m^2/s without adding nanoparticles, and the smallest dry cell weight is 55 μmol/m^2*FACHB-314* cultured with TiO_2 nanoparticles and the control group cultured under TiO_2 nanoparticles (high light intensity is 275 μmol/m^2/s, medium light intensity is 165 μmol/m^2/s, low light intensity is 55 μmol/m^2/s). Figure 9(b) and Table 2 show that the content of phycocyanin in *FACHB-314* decreased slightly with light intensity. This decrement indicates that *A. platensis* is more inclined to accumulate phycocyanin under low light intensity. *A. platensis* cultivated in culture medium with TiO_2nanoparticles or *A. platensis* doped with rGO-TiO_2nanoparticles, the phycocyanin content under low light intensity is higher than the accumulation under high light intensity.

The phycocyanin content was 77.5 mg/g, 75.1 mg/g, and 88.4 mg/g under high light intensity, medium light intensity, and low light intensity, respectively. Compared with the phycocyanin content under high light intensity, the phycocyanin content of *FACHB-314* cultured with nanoparticles under low light intensity increased by 10.9 mg/g, an increase of 6.4%. Therefore, without adding nanoparticles,*FACHB-314* under a low light intensity culture environment is more conducive to the accumulation of intracellular phycocyanin. Under the condition of light intensity of 55 μmol/m^2/s, the highest phycocyanin content is *FACHB-314* cultured with rGO-TiO_2 nanoparticles, and the content value is 89.6 mg/g. Then, the *FACHB-314* cultured in the control group had a phycocyanin content of 88.4 mg/g; the *FACHB-314* cultured with TiO_2 nanoparticles had a phycocyanin content of 69.7 mg/g. *FACHB-314* cultured with rGO-TiO_2nanoparticles increased by 1.4% compared to the *FACHB-314*cultured in the control group and increased by 28.6% compared to the*FACHB-314* cultured with TiO_2 nanoparticles. In terms of phycocyanin production, the largest yield was the*FACHB-314* co-cultured with rGO-TiO_2nanoparticles. Compared with the control group, the yield of phycocyanin increased by 10.6%, and compared with the *FACHB-314* co-cultured with TiO_2 nanoparticles, it increased by 34.2 %.

Figure 10 shows that under the condition of light intensity of 55 μmol/m^2/s, the maximum dry cell weight of the control group is 1.14 g/L, and the dry cell weight yield is 0.113 g/L/d.*FACHB-314* cultured with rGO-

TiO_2 nanoparticle has a maximum dry cell weight of 1.19 g/L and a dry cell weight yield of 0.119 g/L/d. Compared with the control group with the same light intensity, its dry cell weight and dry cell weight yield increased by 4.4% and 5.3%, respectively. Under the light intensity of 165 μmol/m^2/s, the maximum dry cell weight of the control group was 1.73 g/L, and the dry cell weight yield was 0.186 g/L/d.*FACHB-314* cultured with TiO_2 nanoparticles has a maximum dry cell weight of 1.47 g/L and a dry cell weight yield of 0.154 g/L/d. The maximum dry cell weight of *FACHB-314* cultured with rGO-TiO_2 nanoparticles was 1.66 g/L, and the dry cell weight yield was 0.178 g/L/d. Compared with the experimental group added with TiO_2 nanoparticles under the condition of light intensity of 165 μmol/m^2/s, the dry cell weight and dry cell weight yield of *FACHB-314* cultured with rGO-TiO_2 nanoparticles increased by 12.9% and 15.6%, respectively. Under high light intensity, the maximum dry cell weight of the control group was 2.76 g/L, and the dry cell weight yield was 0.320 g/L/d. *FACHB-314* cultured with TiO_2 nanoparticles has a maximum dry cell weight of 2.26 g/L and a dry cell weight yield of 0.258 g/L/d. *FACHB-314* cultured with rGO-TiO_2nanoparticles has a maximum dry cell weight of 2.58 g/L and a dry cell weight yield of 0.298 g/L/d. In the experimental group added with TiO_2 nanoparticles and spirulina cultured with rGO-TiO_2 nanoparticles, the dry cell weight and dry cell weight yield increased by 14.2% and 16.0%, respectively.

The dry cell weight increased by 2.17 times as the light intensity increased from low to high value. It shows that high light intensity is more conducive to the growth of *A. Platensis* FACH-314. High light intensity is compared with low light intensity, Spirulina's photosynthesis receives more photoelectrons per unit of time, which improves photosynthetic efficiency, so it accumulates more organic matter and promotes the growth of *A. platensis* FACH-314.

The results indicate that *FACHB-314* co-cultured with rGO-TiO_2 nanoparticles has higher phycocyanin content than the other two groups. It shows that in the existing culture experiments with different light intensities, the addition of rGO-TiO_2 nanoparticles will promote the accumulation of phycocyanin in *FACHB-314* , and the promotion effect is higher than that of the culture with TiO_2 nanoparticles.

3.6. Effects of Different Light and Dark Cycles on the Growth and Phycocyanin Content of FACHB-314

The light-dark control group chooses full light (lighting time: dark time = 24h: 00h) and half-light time (lighting time: dark time = 12h: 12h) for comparison (Lamminen et al., 2017). During these two periods of light and darkness, adding nanoparticles to *FACHB-314* alters growth. The growth curve in Figure 11(a) shows that different nanoparticles have a certain effect on the growth of *FACHB-314* in a different light and dark periods.

Analyze the growth data of each group of *FACHB-314* . On day 9 of the culture, the dry cell weight and biomass yield results of the three groups of *FACHB-314* are shown in Figure 11(b). In the control group, the dry cell weight of *FACHB-314* under half-light was only 1.00 g/L, while the dry cell weight under full light increased to 1.73 g/L, which was nearly doubled compared to half-light. This indicates that the growth of the spiral depends on the light time, and a longer light time is more beneficial to the growth of *FACHB-314* . This is due to the increased photoreaction time of photosynthesis of*FACHB-314* , which accumulates more organic matter, which promotes its growth.

The effect of rGO-TiO_2 nanoparticles on the growth of three groups of *FACHB-314* under half-light. The growth trend of the experimental group with TiO_2 nanoparticles was like that of the control group, and the biomass of *FACHB-314* with rGO-TiO_2 nanoparticles was higher than that of the control group. The dry cell weight of the control group with nanoparticles added under half-light was 1.00 g/L, and the dry cell weight yield was 0.098 g/L/d. In the medium supplemented with TiO_2 nanoparticles, the dry cell weight of*FACHB-314* reached its maximum value on the ninth day and was 0.90 g/L, and its dry cell weight yield was 0.085 g/L/d. The dry cell weight of *FACHB-314* reached its maximum value on the ninth day of the medium supplemented with rGO-TiO_2 nanoparticles, and it was 1.17 g/L, which was an increase of 17.0% compared with the control group; its dry cell weight yield It was 0.119 g/L/d, which was an increase of 21.4% compared with the control group. Compared with*FACHB-314* with TiO_2 nanoparticles added with rGO-TiO_2 nanoparticles, the dry cell weight increased by 20.0% and the dry cell weight yield increased by

40.0% under half-light. The above results show that under the two different light and dark cycle conditions, the biomass of the experimental group with rGO-TiO_2 nanoparticles is higher than that of the experimental group with TiO_2 nanoparticles, and the growth of *FACHB-314* under half-light is obvious enhancement.

The results in Figure 11(c) and Table 3 show that during the semi-light culture, the phycocyanin content of *FACHB-314* and nanoparticles is always lower than the cumulative amount under the full-light culture. It can be found that *FACHB-314* cultivated with nanoparticles is not conducive to the accumulation of algal protein in the half-light. (c) shows that the maximum intracellular phycocyanin content of*FACHB-314* cultured in the absence of light is 38.7 mg/g, and the yield is 38.70 mg/L. Compared with full light, the content and yield of phycocyanin were reduced by 48.5% and 52.7%, respectively. Similarly, in the two experimental groups where nanoparticles were added, the decrease in phycocyanin content and the decrease in phycocyanin production also had different degrees.

4. Analysis of gene expression related to phycocyanin synthesis by rGO-TiO_2

The regulation of the metabolic synthesis of phycocyanin in*FACHB-314* can be assessed by gene expression level analysis. In this study, we choose three key synthetase enzymes that can regulate the synthesis of phycocyanin: The gene encodes urinary hyaluronan III synthase (CobA-hemG), which can promote the production of urobilin III, which is an important tetrapyrrole intermediate, including the synthesis of chlorophyll, vitamin B12, heme and bilinin (Doan et al., 2021; Faieta et al., 2021). HemG gene encodes protoporphyrinogen IX oxidase, which can catalyze oxidized protoporphyrinogen IX to produce protoporphyrin IX (Li et al., 2017; Lupatini et al., 2017). The gene encodes heme oxygenase (Ho), which catalyzes the opening of the heme ring structure to form chlorophyll IX, an intermediate in the biosynthesis of bilinin (Liu et al., 2019; Rosa et al., 2019). Under the same conditions, compare the control group and the nanoparticle addition experimental group, and evaluate the regulation and influence mechanism of the material on the synthesis of phycocyanin from the gene expression level as shown in Figure 12 (a).

Figure 12 (b) shows the effect of the phycocyanin synthesis and metabolism pathway in *FACHB-314* cells on the gene expression levels of CobA-hemG, HemG and Ho three enzyme proteins after the experimental group and the control group were cultured for 72 hours.

Compared with the control group, the transcript expression levels of CobA-hemG, HemG and ho genes in the *FACHB-314* group containing rGO-TiO_2 composite nanoparticles were significantly higher than those in the control group, which were 7.57, 5.65 and 3.33 times. The significant differences in the transcriptional expression levels of the three key genes in the phycocyanin synthesis pathway can be explained as follows: the mechanism of rGO-TiO_2photocatalytic nanoparticles to promote phycocyanin synthesis in*FACHB-314* cells is by stimulating the overexpression of genes encoding key enzymes in the biosynthetic pathway of phycocyanin, thereby promoting a lot of synthesis of CobA-hemG, HemG, and Ho enzyme proteins during the synthesis and metabolism of phycocyanin. Furthermore, the*FACHB-314* of the experimental group was induced to increase the accumulation of phycocyanin. The results of the difference in phycocyanin gene expression between the experimental group and the control group are consistent with the above results, that is, rGO-TiO_2 photocatalytic nanoparticles can significantly increase the content of phycocyanin in *FACHB-314* under red light conditions. The above results clarify from the level of gene transcription and expression that rGO-TiO_2photocatalytic nanoparticles sequentially promote the synthesis of uroporphyrinogen III, protoporphyrin IX and biliverdin IX intermediates through enzymatic reactions, thereby increasing the synthesis of phycocyanin.

5. Discussion

This topic focuses on the promotion of the addition of rGO-TiO_2 nanoparticles on the growth of *FACHB-314*platensis and the accumulation of intracellular phycocyanin. Through a series of experimental optimization and exploration, the following conclusions are drawn:

In this experiment, we designed and prepared reduced graphene oxide titanium dioxide nanoparticles (rGO-TiO_2) with good biocompatibility, which were used in the cultivation of *FACHB-314*platensis to enhance the

absorption and utilization of light, compared with conventional TiO_2 Nanoparticles, rGO-TiO_2 nanoparticles have high biocompatibility, have no significant inhibitory effect on the growth of *FACHB-314* , and have no obvious damage to the morphology and structure. To study the effects of rGO-TiO_2 nanoparticles on the growth of*A. platensis* and the accumulation of phycocyanin under different irradiation light colors, light-dark cycles, and light intensity conditions.

Under the same conditions, compared with the TiO_2nanoparticles and the control group, the addition of rGO-TiO_2 showed a greater promotion advantage. By the seventh day of culture, the maximum phycocyanin content was 80.3 mg/g, and the intracellular phycocyanin production at 97.16 mg/L, the production of phycocyanin increased by 18.7%. Compared with the*FACHB-314* cultured with TiO_2 nanoparticles, the phycocyanin content increased by 24.6 mg/g compared with the experimental group with TiO_2 nanoparticles, and the content increased by 44.2%. On the ninth day of culture, the cell dry weight reached the maximum value of 1.66 g/L, and $TiO_2$was 0.65 g/L.

We found that in the choice of different wavelengths, the cell growth of*A. platensis FACHB-314* and the accumulation of phycocyanin are more biased towards the white light. Under different light-dark cycles, full light has a more obvious promotion effect on the cell growth of *A. platensis* and the accumulation of phycocyanin. Under different light intensities, we found that high light intensity is more beneficial to the growth of *FACHB-314* , while the accumulation of phycocyanin prefers low light intensity. Compared with the control group cultured without nanoparticles, *A. platensis FACHB-314*doped with rGO-TiO_2 nanoparticles can promote the accumulation of phycocyanin.

Acknowledgments

The authors thank Dr. Keju Jing and Jiao Hu for the critical reading of the manuscript. This work was supported by Ludwig-Maximilians-University Munich Open Access fund and the China Scholarship Council.

Conflict of Interest

The authors declared that they have no conflicts of interest in this work.

Data Available Statement

The data that support the findings of this study are available from the corresponding author P. Xiong, upon reasonable request.

Reference

Akter, T., Hossain, A., Islam, M.R., Hossain, M.A., Das, M., Rahman, M.M., Aye, A.T., Abdel-Tawwab, M. 2021. Effects of spirulina (Arthrospira platensis) as a fishmeal replacer in practical diets on growth performance, proximate composition, and amino acids profile of pabda catfish (Ompok pabda). *Journal of Applied Aquaculture* .

Alagawany, M., Taha, A.E., Noreldin, A., El-Tarabily, K.A., El-Hack, M.E.A. 2021. Nutritional applications of species of Spirulina and Chlorella in farmed fish: A review. *Aquaculture* , **542** .

Almomani, F. 2020. Algal cells harvesting using cost-effective magnetic nano-particles. *Science of the Total Environment* , **720** , 12.

Ambati, R.R., Gogisetty, D., Aswathanarayana, R.G., Ravi, S., Bikkina, P.N., Lei, B., Su, Y.P. 2019. Industrial potential of carotenoid pigments from microalgae: Current trends and future prospects. *Critical Reviews in Food Science and Nutrition* , **59** (12), 1880-1902.

Bajpai, V.K., Shukla, S., Kang, S.M., Hwang, S.K., Song, X., Huh, Y.S., Han, Y.K. 2018. Developments of Cyanobacteria for Nano-Marine Drugs: Relevance of Nanoformulations in Cancer Therapies. *Marine Drugs* ,**16** (6), 23.

Basavarajappa, P.S., Patil, S.B., Ganganagappa, N., Reddy, K.R., Raghu, A.V., Reddy, C.V. 2020. Recent progress in metal-doped TiO2, non-metal doped/codoped TiO2 and TiO2 nanostructured hybrids for

enhanced photocatalysis. *International Journal of Hydrogen Energy* ,**45** (13), 7764-7778.

Benedetti, M., Vecchi, V., Barera, S., Dall'Osto, L. 2018. Biomass from microalgae: the potential of domestication towards sustainable biofactories. *Microbial Cell Factories* , **17** , 18.

Bhalamurugan, G.L., Valerie, O., Mark, L. 2018. Valuable bioproducts obtained from microalgal biomass and their commercial applications: A review. *Environmental Engineering Research* , **23** (3), 229-241.

Buchmann, L., Bertsch, P., Bocker, L., Krahenmann, U., Fischer, P., Mathys, A. 2019. Adsorption kinetics and foaming properties of soluble microalgae fractions at the air/water interface. *Food Hydrocolloids* , **97** , 9.

Caporgno, M.P., Mathys, A. 2018. Trends in Microalgae Incorporation Into Innovative Food Products With Potential Health Benefits. *Frontiers in Nutrition* , **5** , 10.

Dalu, T., Wasserman, R.J., Magoro, M.L., Froneman, P.W., Weyl, O.L.F. 2019. River nutrient water and sediment measurements inform on nutrient retention, with implications for eutrophication. *Sci Total Environ* , **684** , 296-302.

Doan, Y.T.-T., Ho, M.-T., Nguyen, H.-K., Han, H.-D. 2021. Optimization of Spirulina sp. cultivation using reinforcement learning with state prediction based on LSTM neural network. *Journal of Applied Phycology* .

Faieta, M., Neri, L., Di Michele, A., Di Mattia, C.D., Pittia, P. 2021. High hydrostatic pressure treatment of Arthrospira (Spirulina) platensis extracts and the baroprotective effect of sugars on phycobiliproteins.*Innovative Food Science & Emerging Technologies* , **70** .

Ferreira-Santos, P., Miranda, S.M., Belo, I., Spigno, G., Teixeira, J.A., Rocha, C.M.R. 2021. Sequential multi-stage extraction of biocompounds from Spirulina platensis: Combined effect of ohmic heating and enzymatic treatment. *Innovative Food Science & Emerging Technologies* , **71** .

Fu, Y., Chen, T., Chen, S.H.Y., Liu, B., Sun, P., Sun, H., Chen, F. 2021. The potentials and challenges of using microalgae as an ingredient to produce meat analogues. *Trends in Food Science & Technology* ,**112** , 188-200.

Grossmann, L., Hinrichs, J., Weiss, J. 2020. Cultivation and downstream processing of microalgae and cyanobacteria to generate protein-based technofunctional food ingredients. *Critical Reviews in Food Science and Nutrition* , **60** (17), 2961-2989.

Guo, W., Zhu, S., Li, S., Feng, Y., Wu, H., Zeng, M. 2021. Microalgae polysaccharides ameliorates obesity in association with modulation of lipid metabolism and gut microbiota in high-fat-diet fed C57BL/6 mice.*International journal of biological macromolecules* , **182** , 1371-1383.

Hazeem, L.J., Yesilay, G., Bououdina, M., Perna, S., Cetin, D., Suludere, Z., Barras, A., Boukherroub, R. 2020. Investigation of the toxic effects of different polystyrene micro-and nanoplastics on microalgae Chlorella vulgaris by analysis of cell viability, pigment content, oxidative stress and ultrastructural changes. *Marine Pollution Bulletin* , **156** , 10.

He, X.X., Xie, C.J., Ma, Y.H., Wang, L., He, X., Shi, W.Q., Liu, X.D., Liu, Y., Zhang, Z.Y. 2019. Size-dependent toxicity of ThO2 nanoparticles to green algae Chlorella pyrenoidosa. *Aquatic Toxicology* ,**209** , 113-120.

Hong, C., Wang, Z., Si, Y., Li, Z., Xing, Y., Hu, J., Li, Y. 2021a. Effects of aqueous phase circulation and catalysts on hydrothermal liquefaction (HTL) of penicillin residue (PR): Characteristics of the aqueous phase, solid residue and bio oil. *Science of the Total Environment* , **776** .

Hong, W., Chen, J., Ding, Q., Gao, Y., Ye, L., Yin, Y., Tu, S. 2021b. Efficient thermochemical liquefaction of microalgae Haematococcus pluvialis for production of high quality biocrude with high selectivity over Fe/montmorillonite catalyst. *Journal of the Energy Institute* , **97** , 73-79.

Hu, J.J., Nagarajan, D., Zhang, Q.G., Chang, J.S., Lee, D.J. 2018. Heterotrophic cultivation of microalgae for pigment production: A review. *Biotechnology Advances* , **36** (1), 54-67.

Karakas, C.Y., Sahin, H.T., Inan, B., Ozcimen, D., Erginer, Y.O. 2019. In vitro cytotoxic activity of microalgal extracts loaded nano-micro particles produced via electrospraying and microemulsion methods.*Biotechnology Progress* , **35** (6), 8.

Karthikeyan, S., Kalaimurugan, K., Prathima, A., Somasundaram, D. 2018a. Novel microemulsion fuel additive Ce-Ru-O catalysts with algae biofuel on diesel engine testing. *Energy Sources Part a-Recovery Utilization and Environmental Effects* , **40** (6), 630-637.

Karthikeyan, S., Periyasamy, M., Prathima, A. 2020. Performance characteristics of CI engine using Chlorella Vulgaris microalgae oil as a pilot dual fuel blends. *Materials Today-Proceedings* ,**33** , 3277-3282.

Karthikeyan, S., Prabhakaran, T.D. 2018. Emission analysis of Botryococcus braunii algal biofuel using Ni-Doped ZnO nano additives for IC engines. *Energy Sources Part a-Recovery Utilization and Environmental Effects* , **40** (9), 1060-1067.

Karthikeyan, S., Prabhakaran, T.D., Prathima, A. 2018b. Environment effect of La2O3 nano-additives on microalgae-biodiesel fueled CRDI engine with conventional diesel. *Energy Sources Part a-Recovery Utilization and Environmental Effects* , **40** (2), 179-185.

Kashyap, M., Samadhiya, K., Ghosh, A., Anand, V., Shirage, P.M., Bala, K. 2019. Screening of microalgae for biosynthesis and optimization of Ag/AgCl nano hybrids having antibacterial effect. *Rsc Advances* ,**9** (44), 25583-25591.

Keller, M., Reidy, B., Scheurer, A., Eggerschwiler, L., Morel, I., Giller, K. 2021. Soybean Meal Can Be Replaced by Faba Beans, Pumpkin Seed Cake, Spirulina or Be Completely Omitted in a Forage-Based Diet for Fattening Bulls to Achieve Comparable Performance, Carcass and Meat Quality. *Animals* , **11** (6).

Khanra, S., Mondal, M., Halder, G., Tiwari, O.N., Gayen, K., Bhowmick, T.K. 2018. Downstream processing of microalgae for pigments, protein and carbohydrate in industrial application: A review. *Food and Bioproducts Processing* , **110** , 60-84.

Lamminen, M., Halmemies-Beauchet-Filleau, A., Kokkonen, T., Simpura, I., Jaakkola, S., Vanhatalo, A. 2017. Comparison of microalgae and rapeseed meal as supplementary protein in the grass silage based nutrition of dairy cows. *Animal Feed Science and Technology* , **234** , 295-311.

Lebron, Y.A.R., Moreira, V.R., Santos, L.V.S., Jacob, R.S. 2018. Remediation of methylene blue from aqueous solution by Chlorella pyrenoidosa and Spirulina maxima biosorption: Equilibrium, kinetics, thermodynamics and optimization studies. *Journal of Environmental Chemical Engineering* , **6** (5), 6680-6690.

Li, H.K., Zhong, Y.M., Lu, Q., Zhang, X., Wang, Q., Liu, H.F., Diao, Z.H., Yao, C., Liu, H. 2019. Co-cultivation of Rhodotorula glutinis and Chlorella pyrenoidosa to improve nutrient removal and protein content by their synergistic relationship. *Rsc Advances* , **9** (25), 14331-14342.

Li, J.J., Schiavo, S., Rametta, G., Miglietta, M.L., La Ferrara, V., Wu, C.W., Manzo, S. 2017. Comparative toxicity of nano ZnO and bulk ZnO towards marine algae Tetraselmis suecica and Phaeodactylum tricornutum.*Environmental Science and Pollution Research* , **24** (7), 6543-6553.

Liang, Y.M., Kaczmarek, M.B., Kasprzak, A.K., Tang, J., Shah, M.M.R., Jin, P., Klepacz-Smolka, A., Cheng, J.J., Ledakowicz, S., Daroch, M. 2018. Thermosynechococcaceae as a source of thermostable C-phycocyanins: properties and molecular insights. *Algal Research-Biomass Biofuels and Bioproducts* , **35** , 223-235.

Liu, Y.X., Jin, W.B., Zhou, X., Han, S.F., Tu, R.J., Feng, X.C., Jensen, P.D., Wang, Q.L. 2019. Efficient harvesting of Chlorella pyrenoidosa and Scenedesmus obliquus cultivated in urban sewage by magnetic flocculation using nano-Fe3O4 coated with polyethyleneimine. *Bioresource Technology* , **290** , 9.

Lupatini, A.L., Colla, L.M., Canan, C., Colla, E. 2017. Potential application of microalga Spirulina platensis as a protein source.*Journal of the Science of Food and Agriculture* , **97** (3), 724-732.

Lupatini Menegotto, A.L., Fernandes, I.A., Bucior, D., Balestieri, B.P., Colla, L.M., Abirached, C., Franceschi, E., Steffens, J., Valduga, E. 2021. Purification of protein from Arthrospira platensis using aqueous two-phase system associate with membrane separation process and evaluation of functional properties. *Journal of Applied Phycology* .

Madeira, M.S., Cardoso, C., Lopes, P.A., Coelho, D., Afonso, C., Bandarra, N.M., Prates, J.A.M. 2017. Microalgae as feed ingredients for livestock production and meat quality: A review. *Livestock Science* , **205** , 111-121.

Minetto, D., Libralato, G., Marcomini, A., Ghirardini, A.V. 2017. Potential effects of TiO2 nanoparticles and TiCl4 in saltwater to Phaeodactylum tricornutum and Artemia franciscana. *Science of the Total Environment* , **579** , 1379-1386.

Mona, S., Malyan, S.K., Saini, N., Deepak, B., Pugazhendhi, A., Kumar, S.S. 2021. Towards sustainable agriculture with carbon sequestration, and greenhouse gas mitigation using algal biochar. *Chemosphere* ,**275** .

Mustafa, S., Bhatti, H.N., Maqbool, M., Iqbal, M. 2021. Microalgae biosorption, bioaccumulation and biodegradation efficiency for the remediation of wastewater and carbon dioxide mitigation: Prospects, challenges and opportunities. *Journal of Water Process Engineering* , **41** .

Nematian, T., Salehi, Z., Shakeri, A. 2020. Conversion of bio-oil extracted from Chlorella vulgaris micro algae to biodiesel via modified superparamagnetic nano-biocatalyst. *Renewable Energy* ,**146** , 1796-1804.

Nguyen, N.H.A., Padil, V.V.T., Slaveykova, V.I., Cernik, M., Sevcu, A. 2018. Green Synthesis of Metal and Metal Oxide Nanoparticles and Their Effect on the Unicellular Alga Chlamydomonas reinhardtii.*Nanoscale Research Letters* , **13** , 13.

Ozkaleli, M., Erdem, A. 2018. Biotoxicity of TiO2 Nanoparticles on Raphidocelis subcapitata Microalgae Exemplified by Membrane Deformation.*International Journal of Environmental Research and Public Health* , **15** (3), 12.

Patel, A.K., Singhania, R.R., Awasthi, M.K., Varjani, S., Bhatia, S.K., Tsai, M.-L., Hsieh, S.-L., Chen, C.-W., Dong, C.-D. 2021. Emerging prospects of macro- and microalgae as prebiotic. *Microbial Cell Factories* , **20** (1).

Raji, A.A., Alaba, P.A., Yusuf, H., Abu Bakar, N.H., Taufek, N.M., Muin, H., Alias, Z., Milow, P., Razak, S.A. 2018. Fishmeal replacement with Spirulina Platensis and Chlorella vulgaris in African catfish (Clarias gariepinus) diet: Effect on antioxidant enzyme activities and haematological parameters. *Research in Veterinary Science* ,**119** , 67-75.

Ribeiro, D.M., Martins, C.F., Kules, J., Horvatic, A., Guillemin, N., Freire, J.P.B., Eckersall, P.D., Almeida, A.M., Prates, J.A.M. 2021. Influence of dietary Spirulina inclusion and lysozyme supplementation on the longissimus lumborum muscle proteome of newly weaned piglets.*Journal of Proteomics* , **244** .

Rizwan, M., Mujtaba, G., Memon, S.A., Lee, K., Rashid, N. 2018. Exploring the potential of microalgae for new biotechnology applications and beyond: A review. *Renewable & Sustainable Energy Reviews* ,**92** , 394-404.

Rodrigues, L.S., do Valle, A.F., D'Elia, E. 2018. Biomass of Microalgae Spirulina Maxima as a Corrosion Inhibitor for 1020 Carbon Steel in Acidic Solution. *International Journal of Electrochemical Science* , **13** (7), 6169-6189.

Rosa, G.M., Morais, M.G., Costa, J.A.V. 2019. Fed-batch cultivation with CO2 and monoethanolamine: Influence on Chlorella fusca LEB 111 cultivation, carbon biofixation and biomolecules production.*Bioresource*

Technology , **273** , 627-633.

Rosenau, S., Oertel, E., Mott, A.C., Tetens, J. 2021. The Effect of a Total Fishmeal Replacement by Arthrospira platensis on the Microbiome of African Catfish (Clarias gariepinus). *Life-Basel* , **11** (6).

Sathasivam, R., Radhakrishnan, R., Hashem, A., Abd Allah, E.F. 2019. Microalgae metabolites: A rich source for food and medicine. *Saudi Journal of Biological Sciences* , **26** (4), 709-722.

Sendra, M., Yeste, M.P., Gatica, J.M., Moreno-Garrido, I., Blasco, J. 2017. Direct and indirect effects of silver nanoparticles on freshwater and marine microalgae (Chlamydomonas reinhardtii and Phaeodactylum tricornutum). *Chemosphere* , **179** , 279-289.

Sengupta, S., Koley, H., Dutta, S., Bhowal, J. 2018. Hypocholesterolemic effect of Spirulina platensis (SP) fortified functional soy yogurts on diet-induced hypercholesterolemia. *Journal of Functional Foods* ,**48** , 54-64.

Shi, X.L., Zou, J., Chen, Z.G. 2020. Advanced Thermoelectric Design: From Materials and Structures to Devices. *Chemical Reviews* ,**120** (15), 7399-7515.

Shirazi, H.M., Karimi-Sabet, J., Ghotbi, C. 2017. Biodiesel production from Spirulina microalgae feedstock using direct transesterification near supercritical methanol condition. *Bioresource Technology* ,**239** , 378-386.

Sorrenti, V., Castagna, D.A., Fortinguerra, S., Buriani, A., Scapagnini, G., Willcox, D.C. 2021. Spirulina Microalgae and Brain Health: A Scoping Review of Experimental and Clinical Evidence. *Marine Drugs* ,**19** (6).

Thirumdas, R., Brncic, M., Brncic, S.R., Barba, F.J., Galvez, F., Zamuz, S., Lacomba, R., Lorenzo, J.M. 2018. Evaluating the impact of vegetal and microalgae protein sources on proximate composition, amino acid profile, and physicochemical properties of fermented Spanish "chorizo" sausages. *Journal of Food Processing and Preservation* ,**42** (11), 8.

Wang, B., He, Z., Zhang, B., Duan, Y. 2021. Study on hydrothermal liquefaction of spirulina platensis using biochar based catalysts to produce bio-oil. *Energy* , **230** .

Wang, C.C., Lan, C.Q. 2018. Effects of shear stress on microalgae - A review. *Biotechnology Advances* , **36** (4), 986-1002.

Wang, F., Guan, W., Xu, L., Ding, Z.Y., Ma, H.L., Ma, A.Z., Terry, N. 2019. Effects of Nanoparticles on Algae: Adsorption, Distribution, Ecotoxicity and Fate. *Applied Sciences-Basel* , **9** (8), 15.

Wang, L., Zhang, C.B., Gao, F., Mailhot, G., Pan, G. 2017. Algae decorated TiO2/Ag hybrid nanofiber membrane with enhanced photocatalytic activity for Cr(VI) removal under visible light. *Chemical Engineering Journal* , **314** , 622-630.

Wils, L., Leman-Loubiere, C., Bellin, N., Clement-Larosiere, B., Pinault, M., Chevalier, S., Enguehard-Gueiffier, C., Bodet, C., Boudesocque-Delaye, L. 2021. Natural deep eutectic solvent formulations for spirulina: Preparation, intensification, and skin impact.*Algal Research-Biomass Biofuels and Bioproducts* , **56** .

Wu, Z.Q., Yang, W.C., Tian, X.Y., Yang, B.L. 2017. Synergistic effects from co-pyrolysis of low-rank coal and model components of microalgae biomass. *Energy Conversion and Management* , **135** , 212-225.

Ye, C.S., Mu, D.Y., Horowitz, N., Xue, Z.L., Chen, J., Xue, M.X., Zhou, Y., Klutts, M., Zhou, W.G. 2018. Life cycle assessment of industrial scale production of spirulina tablets. *Algal Research-Biomass Biofuels and Bioproducts* , **34** , 154-163.

Yucetepe, A., Saroglu, O., Ozcelik, B. 2019. Response surface optimization of ultrasound-assisted protein extraction from Spirulina platensis: investigation of the effect of extraction conditions on techno-functional properties of protein concentrates. *Journal of Food Science and Technology-Mysore* , **56** (7), 3282-3292.

Yung, M.M.N., Fougeres, P.A., Leung, Y.H., Liu, F.Z., Djurisic, A.B., Giesy, J.P., Leung, K.M.Y. 2017. Physicochemical characteristics and toxicity of surface-modified zinc oxide nanoparticles to freshwater and marine microalgae. *Scientific Reports* , **7** , 14.

Zhan, J., Rong, J.F., Wang, Q. 2017. Mixotrophic cultivation, a preferable microalgae cultivation mode for biomass/bioenergy production, and bioremediation, advances and prospect. *International Journal of Hydrogen Energy* , **42** (12), 8505-8517.

Zhang, C., Chen, X.H., Tan, L.J., Wang, J.T. 2018. Combined toxicities of copper nanoparticles with carbon nanotubes on marine microalgae Skeletonema costatum. *Environmental Science and Pollution Research* , **25** (13), 13127-13133.

Zhou, T., Cao, L., Zhang, Q., Liu, Y., Xiang, S., Liu, T., Ruan, R. 2021. Effect of chlortetracycline on the growth and intracellular components of Spirulina platensis and its biodegradation pathway.*Journal of Hazardous Materials* , **413** .

Zhu, B., Xiao, T., Shen, H., Li, Y., Ma, X., Zhao, Y., Pan, K. 2021. Effects of CO2 concentration on carbon fixation capability and production of valuable substances by Spirulina in a columnar photobioreactor. *Algal Research-Biomass Biofuels and Bioproducts* ,**56** .

Figure legends:

Scheme 1. Schematic diagram of *FACHB-314* cultivation device.

Figure 1. rGO-TiO_2 preparation process

Figure 2. XRD spectra of GO, TiO_2, and composite nanomaterial rGO-TiO_2.

Figure 3. SEM and TEM images of rGO-TiO_2composite nanomaterials

Figure 4. XPS full spectrum and C 1s high-resolution image of GO and rGO-TiO_2

Figure 5. Effects of rGO-TiO_2 nanoparticles on the growth and nitrate consumption of *FACHB-314*

Figure 6. The effect of TiO_2 and rGO-TiO_2 on the morphology and structure of*FACHB-314* , electron microscope image

Figure 7. (a) The influence of different wavelengths on the growth of *FACHB-314* , **(b)** Effects of rGO-TiO_2 at different wavelengths on dry cell weight and biomass productivity of *FACHB-314*

Figure 8. The effect of different wavelengths on the content of phycocyanin

Figure 9. (a) The effect of different light intensities on the cells growth of A. platensis, **(b)** The effect of different light intensities on the content of phycocyanin

Figure 10. The effect of different light intensities on the dry cell weight and biomass productivity of A. platensis FACHB-314.

Figure 11. (a) The influence of different light and dark periods on the growth of *FACHB-314* , **(b)** The Effects of Different Light and Dark Cycles on the Dry Cell Weight and Biomass Productivity of *FACHB-314* , **(c)** The effect of different light and dark periods on the content of phycocyanin

scheme 1

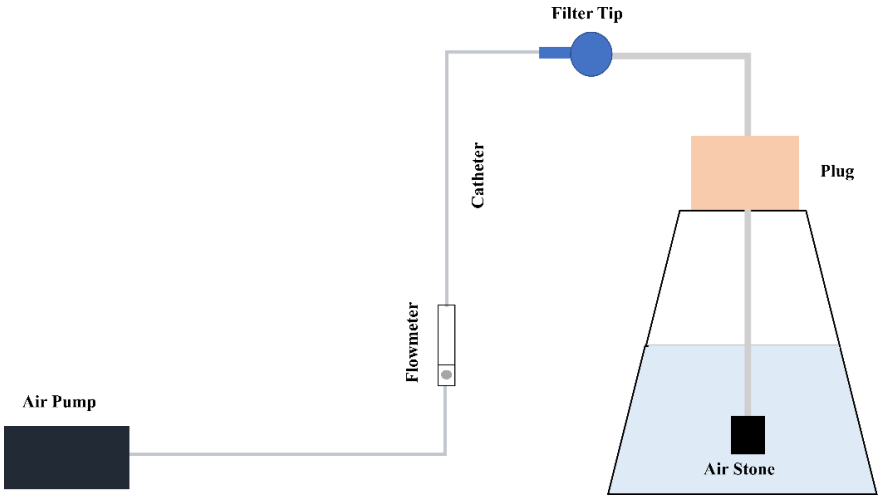

Figure 1

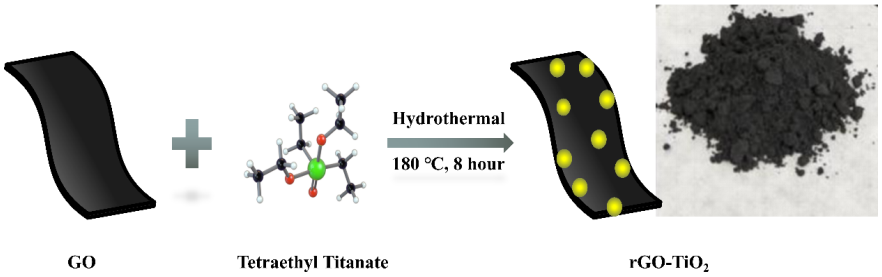

Figure 2

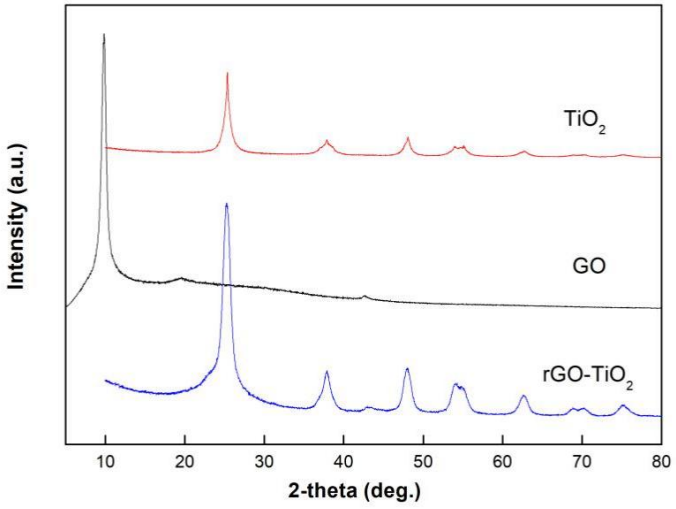

Figure 3

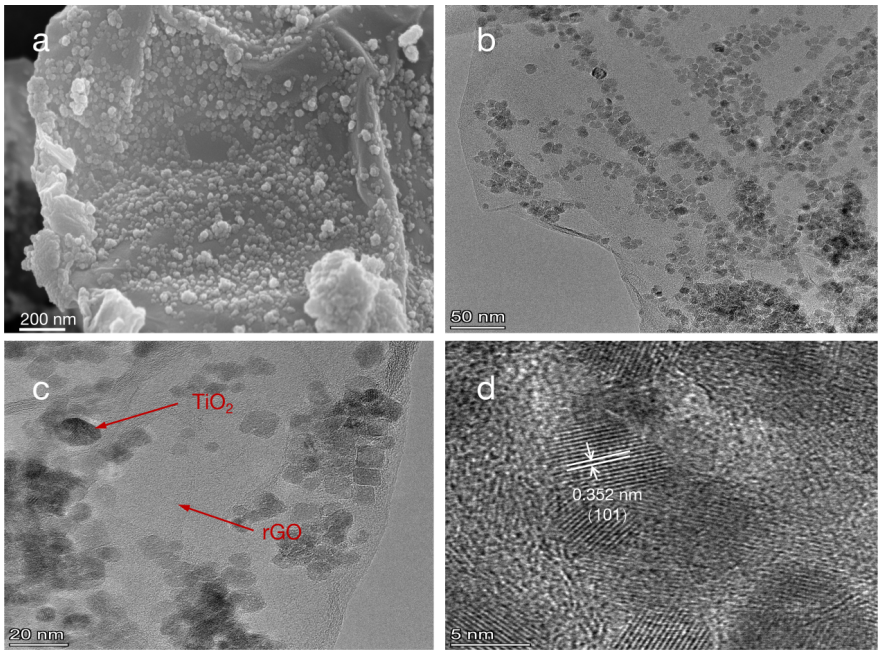

Figure 4

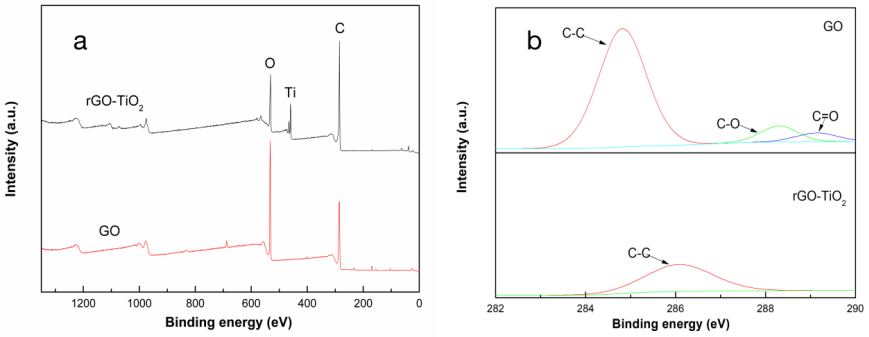

Figure 5

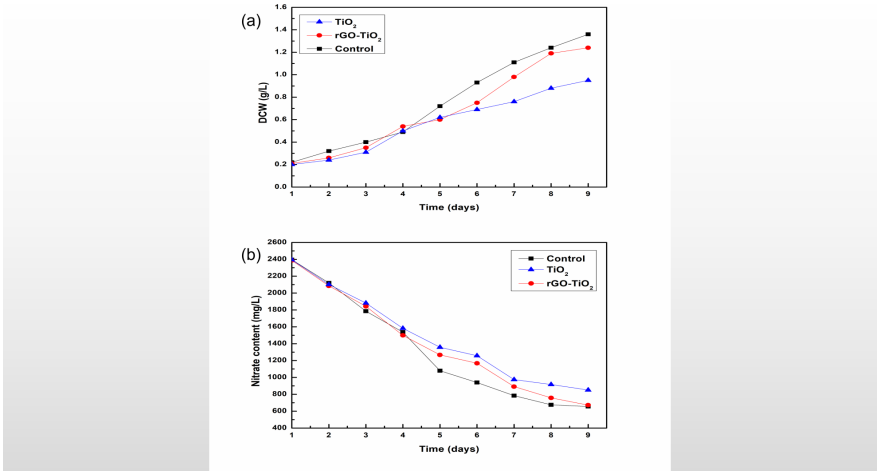

Figure 6

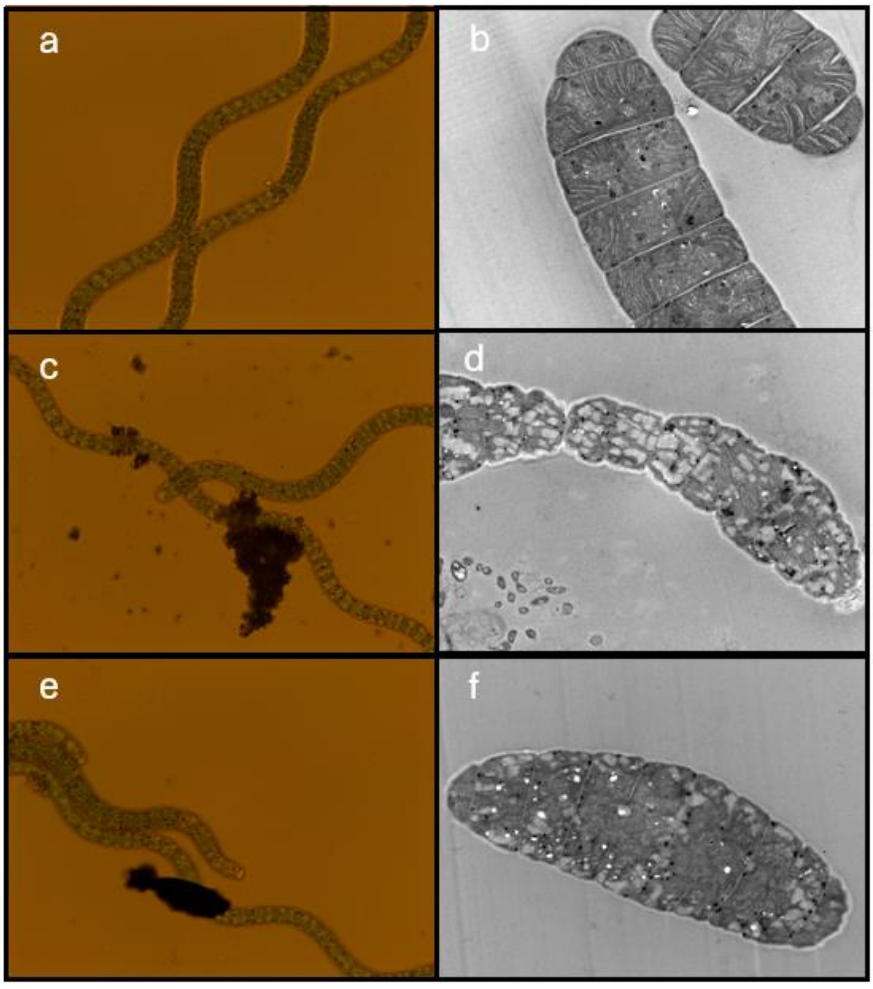

Figure 7

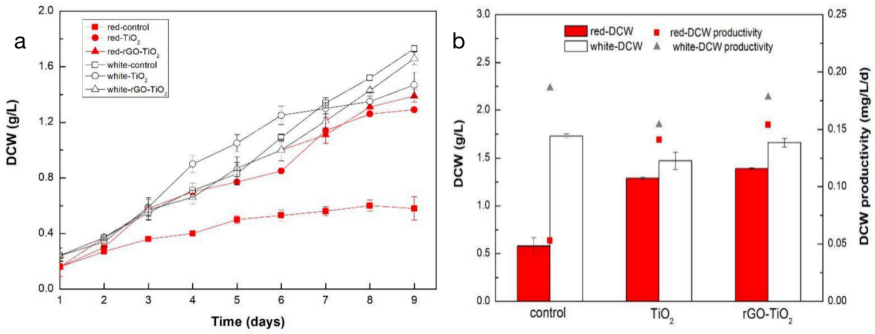

Figure 8

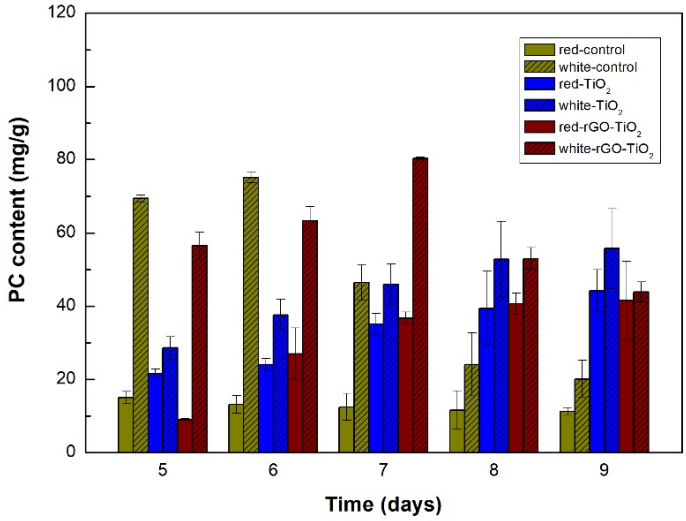

Figure 9

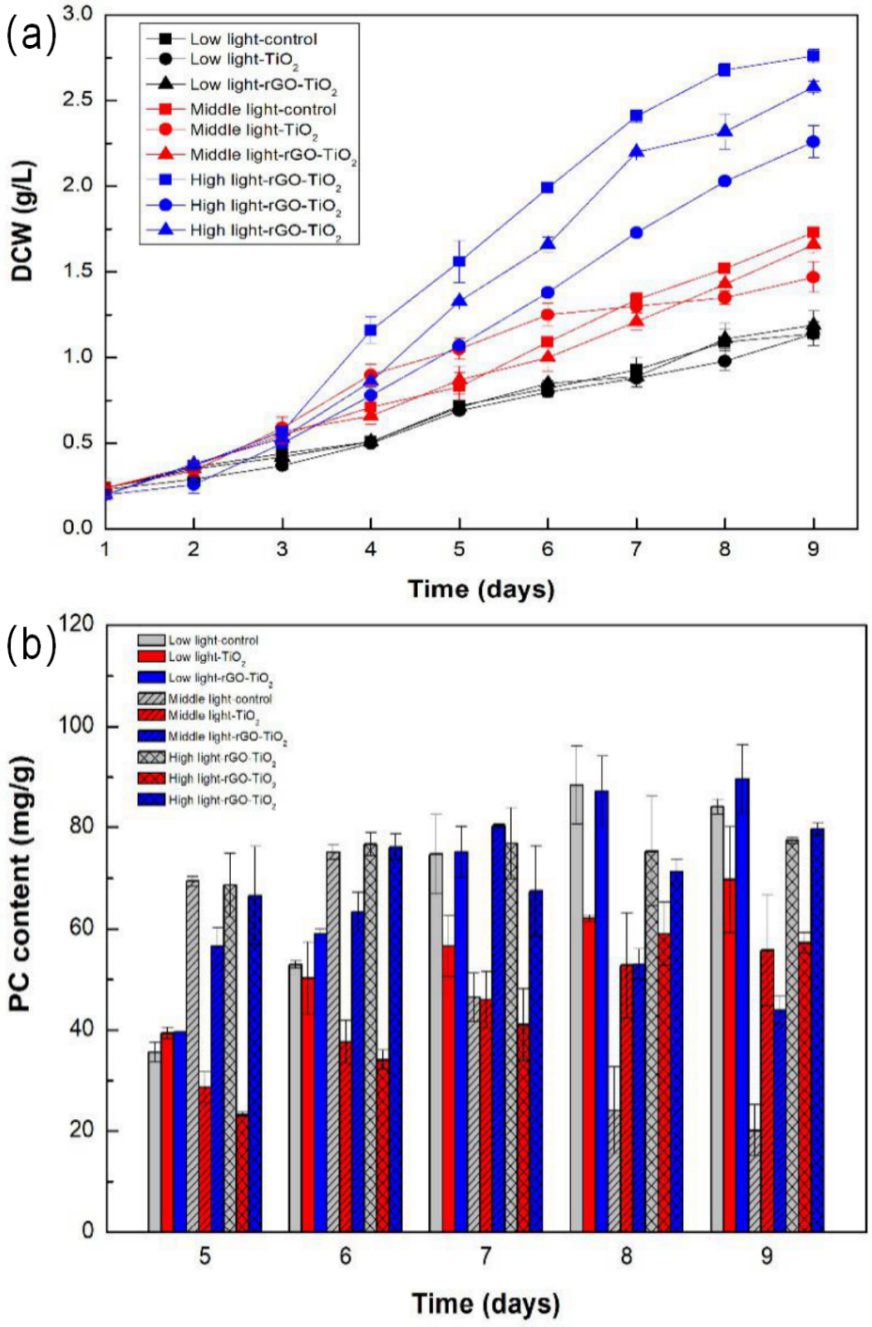

Figure 10

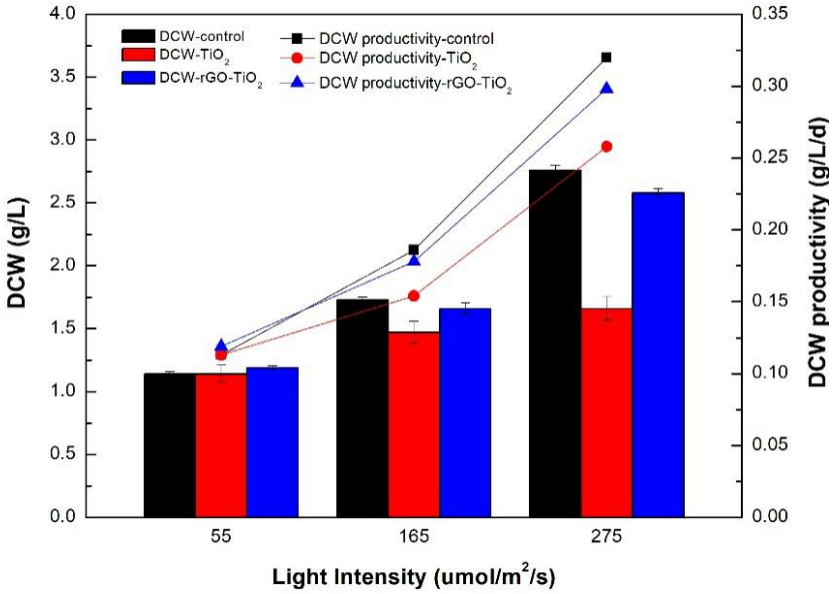

Figure 11

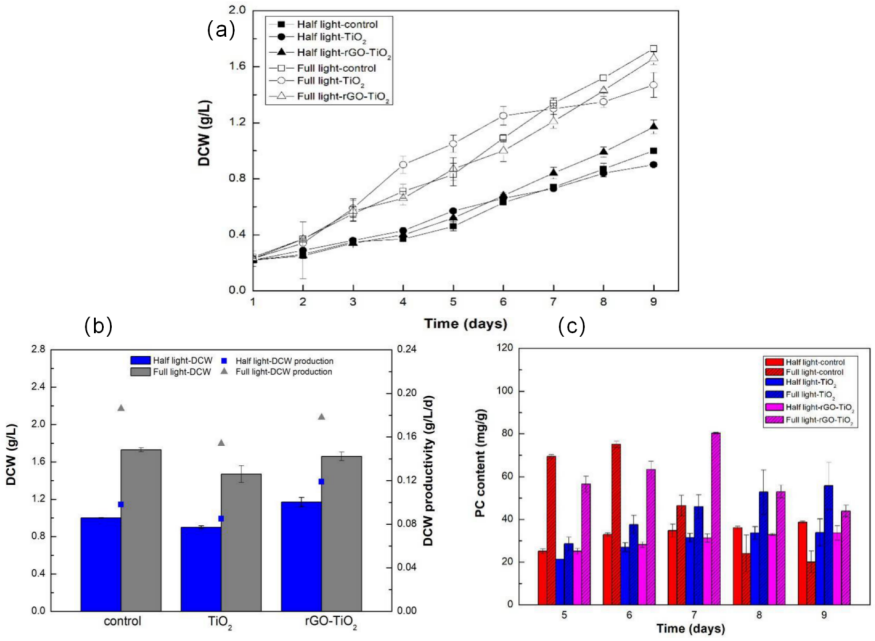

Figure 12

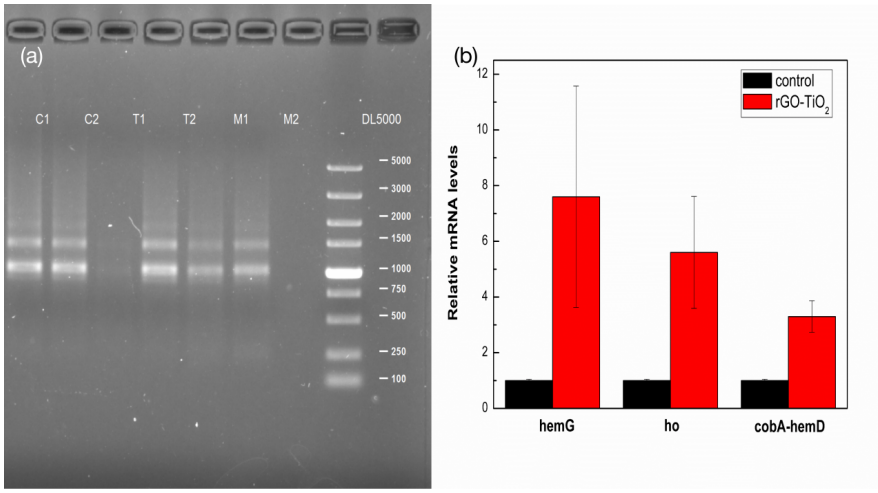

List of tables

Table 1. Cell Biomass, Phycocyanin Content, Phycocyanin Yield of each group at Different wavelengths

Light	**Materials Addition**	**Dry Cell Weight g/L**	**Biomass Productivity g/L/d**	**Phycocyanin Content mg/g**	**Phycocyanin Yield mg/g/d**	**Phycocyanin Production mg/L**
Red	Blank	0.58	0.053	39.0	-	6.24
	TiO_2	1.29	0.141	44.2	0.65	57.02
	rGO-TiO_2	1.39	0.154	52.3	1.66	72.70
White	Blank	1.73	0.186	75.1	4.84	81.86
	TiO_2	1.47	0.154	55.7	2.41	81.88
	rGO-TiO_2	1.66	0.178	80.3	5.49	97.16

Note:

1. The dry cell weight represents the dry cell weight on day 9.
2. The initial values of red light and white light cell dry weight are 0.16 and 0.24, respectively.
3. The initial values of phycocyanin production (mg/g) of each group under red light and white light were 39 and 36.4, respectively.

Table 2. Cell Mass, Phycocyanin Content, and Phycocyanin Yield of each group under Different Light Intensity

Light Intensity	**Materials Addition**	**Dry Cell Weight g/L**	**Biomass Productivity g/L/d**	**Phycocyanin Content mg/g**	**Phycocyanin Yield mg/g/d**	**Phycocyanin Production mg/L**
55 μμολ/μ²/ς	Blank	1.14	0.113	88.4	13.20	96.36
	TiO_2	1.14	0.113	69.7	8.53	79.46
	rGO-TiO_2	1.19	0.119	89.6	13.5	106.62
165 μμολ/μ²/ς	Blank	1.73	0.186	75.1	4.84	81.86
	TiO_2	1.47	0.154	55.7	2.41	81.88

	rGO-TiO_2	1.66	0.178	80.3	5.49	97.16
275 μmoλ/μ²/ς	Blank	2.76	0.320	77.5	2.23	213.9
	TiO_2	2.26	0.258	57.2	-	129.27
	rGO-TiO_2	2.58	0.298	79.7	2.78	205.63

Note:

The dry cell weight represents the dry cell weight on day 9.

The initial values of dry cell weight for low light intensity, medium light intensity, and high light intensity are 0.24, 0.24, and 0.20, respectively.

Table 3. Cell Mass, Phycocyanin Content, Phycocyanin Yield and Phycocyanin Yield of each group under different light periods

Photoperiod	**Materials Addition**	**Dry Cell Weight g/L**	**Biomass Productivity g/L/d**	**Phycocyanin Content mg/g**	**Phycocyanin Yield mg/g/d**	**Phycocyanin Production mg/L**
Semi-illuminated	Blank	1.00	0.098	38.7	3.40	38.7
	TiO_2	0.90	0.085	33.9	2.20	30.51
	rGO-TiO_2	1.17	0.119	33.7	2.20	39.43
Full light	Blank	1.73	0.186	75.1	4.84	81.86
	TiO_2	1.47	0.154	55.7	2.41	81.88
	rGO-TiO_2	1.66	0.178	80.3	5.49	97.16

Note:

The dry cell weight represents the dry cell weight on day 9;

The initial values of cell dry weight in half-light and full-light are 0.22 and 0.24, respectively.